A Beam Tracing Method with Precise Antialiasing for Polyhedral Scenes

Djamchid GHAZANFARPOUR and Jean-Marc HASENFRATZ

Laboratoire MSI - Université de Limoges
E.N.S.I.L.
Technopole F87068 LIMOGES Cedex, France
e-mails: ghazanfa@ensil.unilim.fr   Jean-Marc.Hasenfratz@ensil.unilim.fr

1. Introduction

Ray tracing is one of the most interesting algorithms in computer graphics to generate realistic images of 3D scenes. It is able to simulate various optic phenomena such as shadows, reflections and refractions. However, ray tracing is in essence a point sampling approach (the scene is sampled at the centre of each screen pixel) and thus is prone to the well-known aliasing problems (***image 1***). This is also the case of many other visualization algorithms such as the popular z-buffer [1]. We recall that aliasiasing appears essentialy in the following forms :

- jagged edges;
- discontinuity and/or flash of small objects;
- moiré patterns on textured objects.

Aliasing is a crucial problem for ray tracers because classical antialiasing techniques are inefficient in some cases, in particular for small objects and shadows.

There are two popular antialiasing approaches for ray tracing that use pixel subdivisions and low-pass filterings:

- conventional over-sampling [2, 3] … which is simple and not very expensive;
- stochastic over-sampling [4-6] … whose main advantage is not antialiasing but the simulation of special optical phenomena such as motion blur that cannot be obtained directly [4].

All these over-sampling methods are generally efficient for detecting and antialiasing jaggies but inefficient for other aliasing cases because they cannot guarantee the detection of small objects and small shadows (***images 1***). In fact, there is no correct way to detect small objects and small shadows that slip through the infinitesimal rays or even sub-rays. In order to detect all these problems, the infinitesimal ray concept must be replaced inevitably by a "ray" having some volume called a *beam*.

Beam tracing [7-11] can be considered as an alternative to ray tracing. The antialiasing property of beam tracing is very interesting because it is probably the only approach that can produce a general antialiasing. However, the main goal of most beam tracing methods has not often been the improvement of antialiasing.

The method presented here describes a high quality beam tracer with general and precise antialiasing that extends and improves on the beam tracer for polygonal scenes previously developed by one of the authors [11].

In particular, scenes are modeled by polyhedra instead of polygons, an important improvement based on regular spatial subdivision is used and non-punctual light sources with soft shadows, without any stochastic sampling, are possible.

In our approach the recursive image space subdivision principle is similar to the one used to remove hidden surfaces in [12]. The beams have pyramidal, semi-pyramidal, or pseudo semi-pyramidal shapes. They may appear similar to the beams of [8] but, here, no complex computation of **beam-object intersections** or of **3D polygon clippings** is necessary. This gives out the main advantage of this method over the others of the beam tracing family. In addition to a substantial run time reduction, the absence of complex computations as beam-object intersections or 3D clippings, allows to extend this approach to some non-polyhedral scenes such as CSG ones.

In this method, beams can be considered just as bounding volumes essentially used for the detection of aliased edges, small objects and shadows. After the detection of the aliased regions, a ray tracing with an adaptive over-sampling and a low-pass filtering is used for rendering the regions with antialiasing. Texture antialiasing is handled separately with no over-sampling as we will see later in section 3.2.2.

All aliasing problems, including small objects and small shadows, are precisely detected and solved. Refractions are free from linear approximation or complex computations usually used in similar beam tracers [8, 10]. Soft shadows due to non-punctual light sources can be produced with no stochastic sampling. Well-known improvements of classical ray tracing (spatial subdivisions and hierarchical bounding volumes) are entirely compatible with this beam tracer.

The first part of this paper concerns beam tracing of polyhedral scenes with reflection, refraction and hard shadows. The second one proposes a technique to simulate soft shadows, and the last part presents some results and time comparisons.

2. Method description

In a previous paper [11], we developed a beam tracing method for scenes modeled by any kind of polygons. Now, we study a beam tracing method for scenes modeled by convex polyhedra. The choice of convex polyhedra, corresponding to a great number of scenes, is motivated by a computational argument. In fact, our approach is compatible with concave polyhedra but the detection of aliased regions, in the case of convex polyhedra, is faster because simpler tests can be used to determine the position of objects relative to beams.

The beam tracer is improved by the implementation of spatial subdivision in order to take advantage of the spatial coherence. Two types of spatial subdivisions can be used: regular [13-15] … and irregular [16-18]. In the general case, we did not find any significant advantage between these two approaches for ray tracing in the literature. For example, the conclusion of a recent paper [19] comparing these two kinds of subdivisions is: « *A general statement concerning the question whether ray-generators for octrees lead to better results then ray-generators for uniform subdivisions cannot be made. This will always depend on the chosen scene* ». In addition, the implementation of the regular subdivision is easier than the implementation of the irregular subdivision in the case of beam tracing. For these reasons, we chose a regular spatial subdivision to improve our beam tracer.

We will see principles and conceptual step details of this beam tracer in the following sections.

2.1 Detection of aliased regions

The beams are used to determine two types of image regions:

- *uniform* regions with no aliasing problem concerning jaggies, small objects and small shadows (remember that texture antialiasing problems are handled separately);
- *ambiguous* regions with possible aliasing problems.

2.1.1 Case of opaque and non-reflecting objects

Vision beams

Our method is based on an adaptive recursive subdivision of the image space. First, a region corresponding to the entire screen and its associated vision beam are tested and recursively subdivided until either an *uniform* region is obtained or the pixel subdivision limit is reached. A *vision beam* (primary beam) is a pyramid, traced from the eye to the scene *(**figure 1**)*. This pyramid is defined by the eye (its *apex*) and four rays (its *edges*) passing through the corners of an image region. If the region is ambiguous, it is subdivided in four and four new sub-pyramids are traced.

To determine the type of an image region (uniform or ambiguous), we attach to each edge of its beam the first intersected object†, if this object exists. We can consider four cases of edge-object intersections:

† The computation of edge-object intersections is improved by the use of a classical spatial regular subdivision.

1. there is at least one edge-object intersection but all edges do not intersect the same object (***figure 2.a***);
2. all edges intersect the same object but not the same side of the object (***figure 2.b***);
3. all edges intersect the same side of the same object (***figure 2.c*** or ***2.d***);
4. there is no edge-object intersection (***figure 2.e*** or ***2.f***).

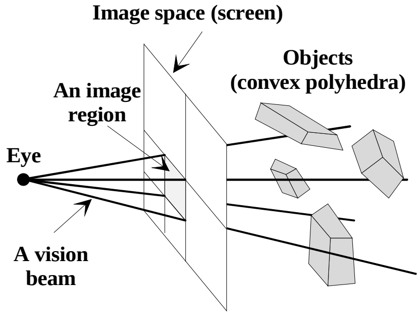

Figure 1 : *Adaptive recursive image subdivision and vision beams.*

Remark: we note that at each subdivision step, we take advantage of the edge-object intersection computed at the previous steps. In particular, the four intersections corresponding to the four common edges are not recomputed.

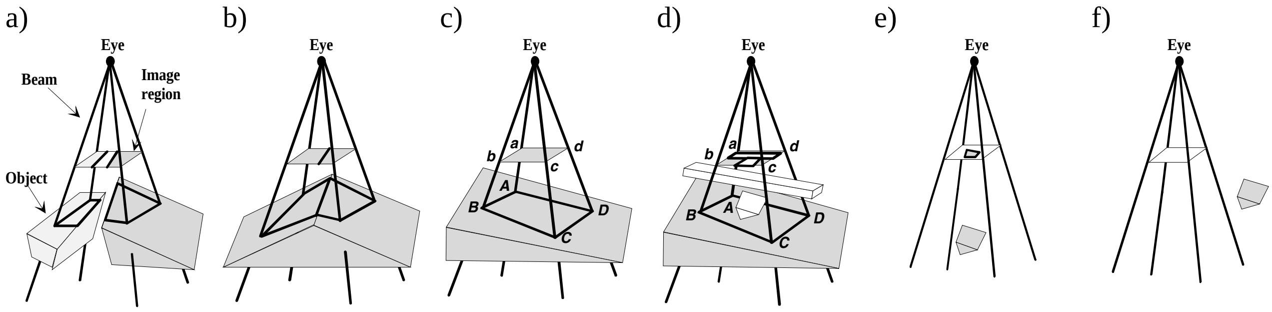

Figure 2 : *Examples of edge-object intersections.*

Cases 1 and 2:

In the first two cases, there is at least one polyhedral edge visible inside the beam (***figure 2.a*** or ***2.b***). So, the region is obviously ambiguous (potential aliasing problems) and further subdivisions are necessary.

Case 3:

This case can be subdivided in two subcases:

- there is no visible polyhedral edge inside the beam (***figure 2.c***), the region is uniform and no subdivision is required;
- there is at least one polyhedral edge visible inside the beam (***figure 2.d***), the region is ambiguous and further subdivisions are required.

Thus, the problem is to find whether or not the truncated beam *abcdABCD* contains or intersects an object. In the context of a shadow-testing acceleration scheme for ray tracing, [20] proposed a sophisticated mixed solution using regular spatial subdivision and octrees. But this solution is very dependent on the beam base size as well as the number and the size of the objects it contains and in some cases, it is very time consuming. We have preferred to use only the well-known regular spatial subdivision in which each voxel (subspace) is associated to a list of its intersecting polyhedral objects. The idea is to find the voxels that are entirely or partially located in the beam and their associated lists of objects in order to position each object relatively to the beam. To make our choice, we compared the run time of several approaches. We chose an approach based on a 3D extension of the conventional scan line algorithm for convex polygon filling. The voxel traversal is done following slices perpendicular to one of the three main axes. Each slice is delimited by the bounding parallelepiped of all the voxels that are intersected by the beam edges (***figure 3***). These beam edges are defined by using a 3D extension of Bresenham's algorithm.

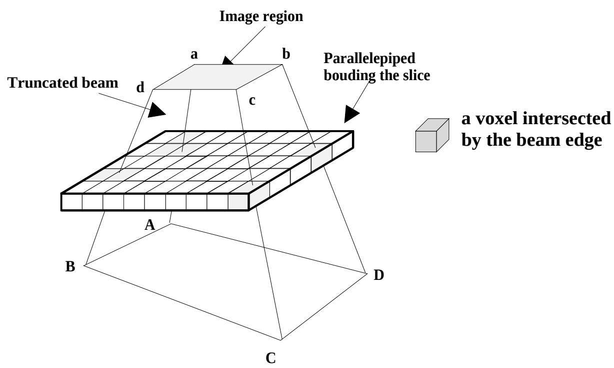

***Figure 3**: Slice delimited by the bounding parallelepiped of all voxels intersected by the beam edges.*

For each traversed voxel, we position its associated objects relatively to the beam. To determine that an object is outside a beam, we use the following rule: if there is a plane that separates the space in a half-space that contains completely the beam and a half-space that contains completely the object, then the object is outside the beam. Judicious separating planes are:

- the image plane *(**figure 4.a**),*
- the plane containing *ABCD, (**figure 4.b**),*
- one of the four sides planes of the beam *(**figure 4.c**),*
- all planes tangent to a beam edge that contains $\vec{e}$ and $\vec{v} = \vec{E} \times \vec{e}$ *(**figure 4.d**)* where $\vec{E}$ is a vector parallel to one edge direction of the polyhedron.

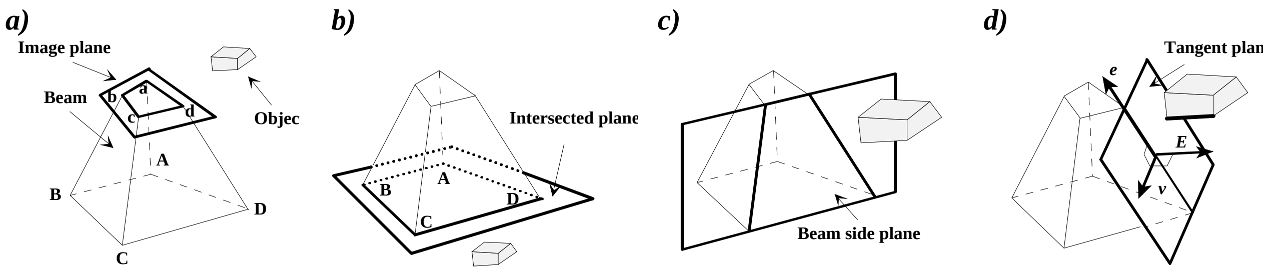

***Figure 4**: Judicious separating planes.*

All these planes are considered in the order of the enumeration. If one of these planes matches the previous rule, the considered object is outside the beam and we test the next object. If all considered objects are outside the beam, there is no aliasing problem *(**figure 2.c**)*, the region is uniform and no more subdivision is required. In other cases, the beam may contain or intersect an object, so the region corresponding to the beam is considered as ambiguous and more subdivisions are required *(**figure 2.d**)*.

Case 4:

This case (***figure 2.e** or **2.f***) is similar to the previous one (***figure 2.c** or **2.d***) if we can "bound" the beam. For this goal, we chose a virtual plane that represents the scene "background". This virtual plane is parallel to the image plane and contains the furthest corner of the regular spatial subdivision from the eye (***figure 5***).

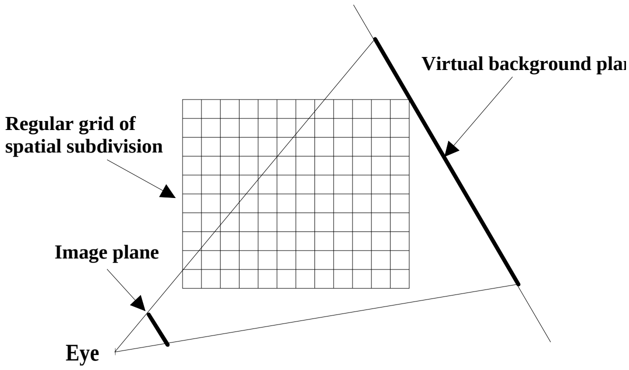

***Figure 5**: 2D representation of the regular spatial subdivision and the virtual background plane.*

Shadow beams:

When the previous tests lead to an uniform region, then the corresponding vision beam entails no further subdivision. This means that only one side of a polyhedron is visible in the beam. The intersection *ABCD* of this side with the beam (***figure 6***) is used to produce a *shadow beam* (secondary beam). A shadow beam is a pyramid that has *ABCD* as its intersection and a light source *S* as its apex *(**figure 6**)*. The visibility of *ABCD* from *S* is determined by new tests. These tests are similar to those used for the vision beam. We need to distinguish among the three following cases*:*

1. *ABCD* is entirely visible from *S* and thus directly illuminated;
2. *ABCD* is entirely hidden from *S* and thus inside the shadow;
3. *ABCD* is partially visible from *S*.

In the first two unambiguous cases, no subdivision is required and a new light source, if it exists, with its corresponding beam, is tested. In the third case, the image region corresponding to *ABCD* is subdivided. We may notice that, in this case, there is no visibility test to perform for the new four vision sub-beams. We must only test the produced shadow sub-beams to determine the visibility of their intersections. Finally, a region is considered uniform in this step if its vision beam and all its shadow beams are uniform. We remark that the tests used for shadow beams are simpler than those used for vision beams. In fact, for an object placed between *S* and *ABCD* and intersecting the four edges of the shadow beam (see ***cases 2*** and ***3*** of vision beam and ***figure 2.b, 2.c*** and ***2.d***), the previous tests concerning the detection of an other object possibly partially or entirely inside the beam are not necessary.

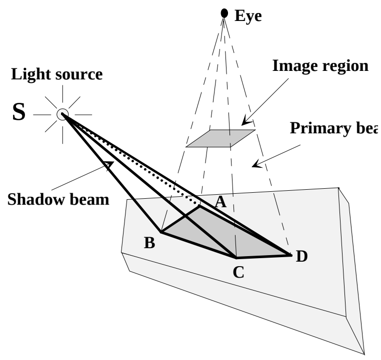

***Figure 6:** Shadow beam.*

2.1.2 Case of reflected and refracted objects

We first studied principles of beam construction and adaptive recursive subdivision for opaque polyhedra without reflection. The natural extensions of this beam tracer to the cases of reflecting and refracting polyhedra will now be studied. These cases concern only regions detected as uniform by vision and shadow beams. For the other regions, where the limit of subdivision is achieved, we go directly to the rendering process (see ***section 3.2***).

Reflections:

The well-known concept of *virtual eye*, as presented among others in [8], is used to compute reflection effects. The virtual eye is the point symmetric to the eye relatively to a reflecting side *R* of a polyhedron *(**figure 7**)*. If *ABCD* is the intersection of a vision beam with this side, a new pyramidal volume can be produced with the virtual eye as its apex and *ABCD* as its intersection *(**figure 7**)*. The *reflection beam* is the upper side of this volume corresponding to a semi-pyramid *(**figure 7**)*. This semi-pyramid is tested in a similar way as a vision beams. If at least one polyhedron edge is visible (entirely or partially) inside the reflecting beam, then the beam subdivision is performed.

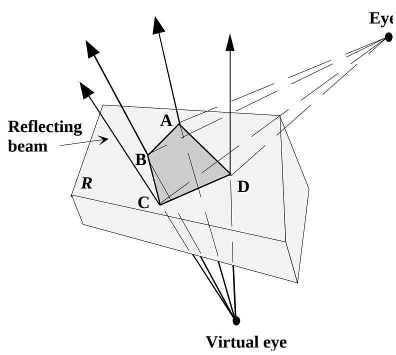

***Figure 7:** Reflection beam.*

Refractions:

Because refraction is not a linear transformation, computing a realistic refraction is a task that cannot be handled correctly using most existing beam tracing algorithms. For example, refraction computations are approximations when using the method developed in [8], in which two different refraction cases are considered. In the first case, the eye is supposed to be positioned far away from the scene; therefore refracted rays are almost parallel. In the second case, the angles of the rays are less than a certain value; in this limited case the refraction can be considered as a linear transformation. So, refracted rays are supposed to converge to a certain point called virtual eye. A more precise, but more complicated refraction determination is developed in [10]. We use a different approach in order to avoid these approximations and complex computations.

Consider *ABCD*, the intersection of a vision beam with a refracting polyhedron *(**figure 8.a**)* and the refracted rays r_1 , r_2, r_3 and r_4 in *A, B, C* and *D (**figure 8.b**)*. Each edge of *ABCD* with a refracted ray can form a plane. For example, there are two refracted rays r_2 and r_3 for edge *BC* and two potential planes P_1 and P_2 produced by *BC* and one of the rays *(**figure 8.b**)*. One of the planes (P_2 in this example) is between *ABCD* and the other one. We choose the outer plane (P_1 in this example) and the three other similar planes to construct a refraction volume. Thus, a *refraction beam* (pseudo semi-pyramid) can be produced by *ABCD* edges and the four planes *(**figure 8.c**)*. This beam contains all the refracted rays concerned by *ABCD*. This beam is tested and may be subdivided in the same way as the previous case. We note that we use at least two refraction beams to traverse the polyhedron ***(figure 8.d)***. More beams are used if the beam exits by more than one face because of an edge aliasing problem (***figure 8.e***). As with previous types of beams, this refraction beam can be considered as a bounding volume for refracted rays and it is only used to detect possible aliased corresponding regions, but the color computations only depend on the refracted rays in the same way as the classical ray tracing (***section 3.2***). So, with our beam tracer refraction computations are as precise as the ray tracers.

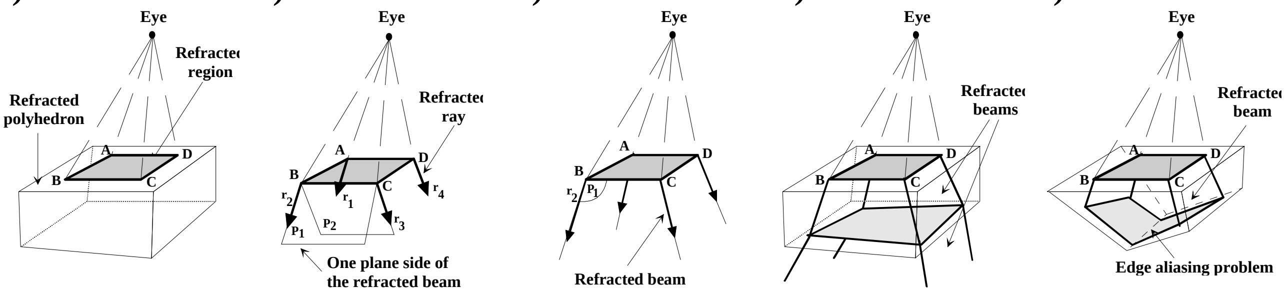

***Figure 8**: **a:** Refraction region, **b** and **c:** plane selection for construction of refraction beam, **d** and **e:** multiple refraction beams.*

2.2 Rendering

2.2.1 Color computations

The goal of the previous sections was the detection of edges, small objects and small shadows corresponding to ambiguous regions and an adaptive recursive subdivision of these regions until uniform regions or the pixel subdivision limit were achieved. A region is detected as uniform when all corresponding beams are tested and when there is no visibility ambiguity inside of them. In order to reach this goal, we have used a variety of beams and have mentioned that these beams are bounding volumes only used to determine the type (ambiguous or uniform) of regions. The color computation in an image region is accomplished by ray tracing. In addition, ray-object intersection computations are improved in this case because intersected objects are already known by the help of associated region beams. Two kinds of regions can be distinguished: regions greater than one screen pixel, regions smaller than one pixel.

In the first case, an uniform region corresponds to one or several pixels. Four rays passing through each pixel corner are traced. We remark that with this method, each ray is common to four neighbour pixels and it is not actually more expensive than tracing rays through pixels centres. The color of a pixel is the average of colors achieved by the four rays. There are two advantages when using four rays per pixel instead of one as in the case for the ray tracing. The first one is a better information representation that can avoid minor aliasing problems as it can be the case with specular reflections. The second one is a more natural and easier implementation of the algorithm specially with texture antialiasing (***section 3.2.2***).

In the second case, we trace a ray through the middle of the sub-pixel. The final color of a screen pixel is the weighted average of the sub-pixels inside the low-pass filter kernel.

2.2.2 Texture antialiasing

Texture mapping as well as 3D texturing in real cases do not fail to produce a texture compression due to perspective projection [21]. Texture compression corresponds to an increase of texture high frequencies and consequently aliasing (specially well-known “moiré” patterns). When using ray or beam tracing methods, there are two possible approaches for texturing with antialiasing.

The usual approach is over-sampling in which pixel subdivision is required not for jagged edge pixels or small objects but inside textured pixels. Two fundamental disadvantages of this approach are persistence of some “moiré” patterns and considerable increase of run time. The first problem is due to the fact that even if an important subdivision rate is used, “moiré” patterns are always noticeable when texture is highly compressed. Run time increase is due to pixel subdivision with one ray per sub-pixel and consequently a greater number of ray-object intersection calculations and texture access.

In the case of texture mapping, efficient prefiltering methods based on the well-known pyramidal structure texture mapping [22] are more interesting than over-sampling. These methods use prefiltered versions of 2D texture corresponding to all possible texture compressions. We can use a method of this type [23] in which the local texture compression in each image pixel is used to choose the corresponding prefiltered texture versions. The notion of texture compression can also be used in the case of some 3D textures as presented in [24, 25]. Our beam tracer is well adapted to these 2D or 3D texturing methods because the texture compression can be achieved without any additional costs (***figure 9***), simply by comparing the size of an image pixel (*abcd*) to the size of its corresponding pyramid intersection with a textured polyhedron side (*ABCD*).

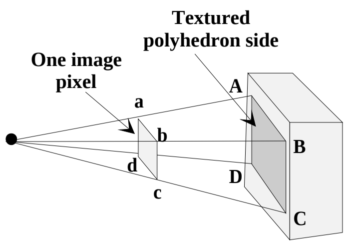

Figure 9: *Texture compression.*

3. Extending beam tracer to compute soft shadows

As described in [26], several techniques exist to compute soft shadows:

- classical techniques based on stochastic ray tracing as [4] are very expensive for large light sources;
- the cone tracing developed in [7] provides soft shadows for spherical light sources but requires complex computations of cone-object intersections.

In this section, we present a method using spherical light sources with our beam tracer to compute realistic, but not real, soft shadows effects. Soft shadows obtained by this method are graphically similar to those obtained by a stochastic ray tracing for small light sources. In addition, in our approach, very large sources can be used to produce realistic soft shadows.

3.1 Basic technique

The effects of soft shadows on a region are due to the absorption of a portion of the light source energy sent by a non punctual light source toward an object region. Our approach has two steps:

- The first step is to detect the regions located in soft shadows. We use particular beams (***see section 4.2***) to identify the regions entirely located in the light, those entirely located in the shadow and those located in the soft shadow.

- The second step is to approximate for each pixel of a soft shadow region the amount of received light energy. We use a beam which has the pixel as its base and contains the light source.

3.2 Detecting soft shadow regions

The idea is similar to the case of punctual light sources: we use a beam to determine problematic regions (regions in soft shadows). To determine these soft shadow regions, for each region *ABCD* (***figure 10.a***) that was detected as uniform by the vision, reflection and refraction beams, we build a *soft shadow beam*. The base of this beam is *ABCD*, its four sides are defined as tangent planes to the spherical light source and its top is the plane *P* (***figure 10.a***). *P* is a plane tangent to the spherical light source with a normal vector *n* approximately (***figure 11***) directed toward the centre of *ABCD*.

Such a beam is an approximation of the light beam coming from the source and reaching the *ABCD* region. Although the soft shadow beam is slightly larger than the beam emitted in reality, our graphical results demonstrate that it fits to a realistic rendering of soft shadows.

The soft shadow beam is then used, with similar tests as those used for the vision beams, to determine the type of a region *ABCD*: entirely in the shadow, entirely lighted or in the soft shadow.
In the first two cases, the region is considered uniform and no subdivisions are necessary. For a lighted region (***figure 13.a***), pixel rendering computations are similar to the point light source (***section 3.2.1***). In fact, in this case, the spherical light source is approximated by a point source of the same energy placed in the center of the sphere. For a region entirely in shadow (***figure 13.d***), pixel rendering computations are identical to the point light source (***section 3.2.1***).
In the third case, the region is subdivided. The recursive subdivision technique of the region and its corresponding soft shadow beams are similar to the case of vision beam. The base of each sub-beam is one of the four sub-regions of *ABCD*, its sides are defined as tangent planes to the spherical source and its top *P'* (***figure 10.b***). *P'* is obtained in the same manner as the plane *P*. The recursive subdivision is continued until a uniform (entirely lighted or entirely shadow) region is obtained or the size of one pixel is reached.

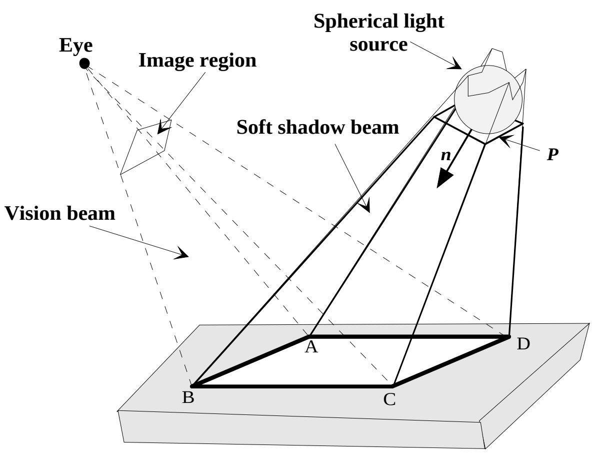

Figure 10.a*: Shadow beam.*

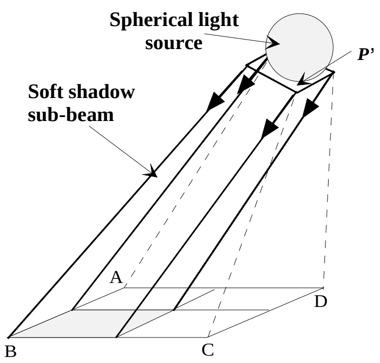

Figure 10.b*: Subdivision of a shadow beam on a region strictly larger than one pixel.*

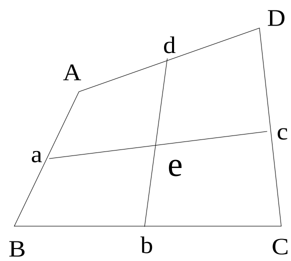

Figure 11*: Approximation of the center of a polygon* ABCD. a *(resp.* b*,* c *and* d*) is the middle of* $\overline{AB}$ *(resp.* $\overline{BC}$, $\overline{CD}$ *and* $\overline{DA}$*). The center e is define as the intersection of* $\overline{ac}$ *and* $\overline{bd}$.

3.3 Portion of light received by the pixel

We are now left with soft shadow regions that are equivalent to a pixel, and for which we can thus evaluate the portion of received light: we recursively divide the beam into four sub-beams (***figure 12***) until we reach an uniform region or the limit of pixel subdivision. The base of a sub-beam is defined like the previous case, its sides are defined as to divide *P'* in four polygons which have approximately‡ the same surface (***figure 12***). For example, we consider the case of the partially illuminated pixel of ***figure 13.b*** and its corresponding beam. This pixel and *P'* are recursively subdivided. Finally, the illumination of the pixel is determined as the sum of illuminated sub-pixels surfaces. This sum approximates the portion of light received by the pixel. ***Figure 13*** shows the different steps of a light soft transition: from an entirely illuminate pixel to a pixel entirely in shadow.

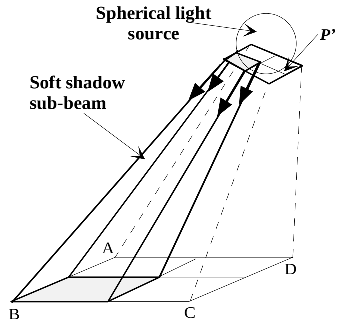

***Figure 12**: Subdivision of a shadow beam on a region smaller than one pixel*

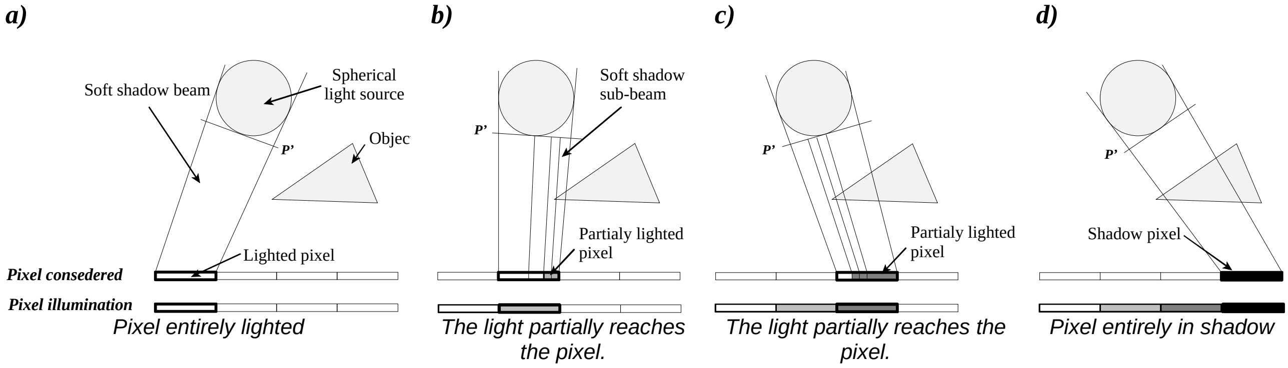

***Figure 13:** Soft shadow example in 2D: illumination of consecutive pixels*

We note that for the smallest sub-pixels (limit of subdivision), the illumination computations are similar to the point light source (***section 3.2.1***). In fact, in this case, the spherical light source is approximated by a point source of the same energy placed in the center of the top polygon (***figure 11***) of the soft shadow beam.

4. Results and comparisons

To compare our beam tracing with the ray tracing, we have used four different test scenes. One scene is produced automatically by random placement of 2060 cubes. Two other scenes are more realistic and represent a room (***images 1 and 2***) and a virtual town (***image 3***). The last scene represents seven pillars and is used for producing soft shadows (***image 4***).

4.1 Aliasing problems and special effects

As we see in ***image 1,*** the problem of small objects and small shadows is entirely solved by our beam tracing. In fact, ray tracing algorithm cannot solve the problem even with an adaptive over-sampling (8x8 rays/pixel): some small objects and small shadows are missed. ***Image 2*** shows different possible effects as reflection, refraction and soft shadows with our beam tracing. We remember that the refraction produced by this method is as precise as the ray tracing algorithm (without approximations used with other beam tracers).

4.2 Computational time

For time comparisons, we have used two scenes: a random placed cubes (2060 polyhedra) and the virtual town of ***image 3*** (1519 polyhedra) in the two following cases:

‡ To divide a polygon into four regions with approximately the same surface, we use the definition of the center of a polygon proposed in ***figure 11***.

In the first case, we have compared ray tracing and beam tracing for the most common image resolution (1024x1024 pixels) with no pixel subdivisions (no antialiasing) and for different regular spatial subdivision sizes.

Result are presented in ***figures 13.a and 13.b***. We see that the best computational time for ray tracing as well as beam tracing is obtained for the regular spatial subdivision of 70x70x70 in which the first algorithm is between 1.5 and 2 times faster than the second one.

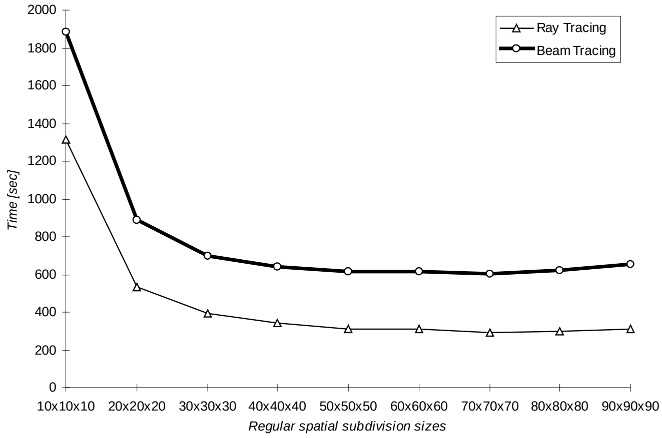

a: *Virtual town (1519 polyhedra).*

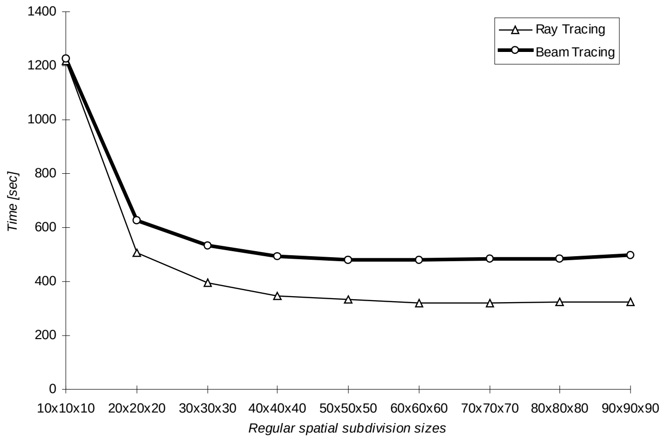

b: *2060 random placed cubes.*

Figure 13*: Time comparison between the ray tracing and our beam tracing for different regular spatial subdivisions for a 1024x1024 pixels image with no pixel subdivisions (no antialiasing).*

In the second case, we have compared ray tracing and beam tracing for the a 1024x1024 pixels image resolution with different pixel subdivisions and for a regular spatial subdivision size of 70x70x70. Result are presented in ***figures 14.a and 14.b***. In each case, the maximal adaptative pixel subdivisions for beam tracing are limited to the overall pixel subdivisions for ray tracing.

To obtain a similar image quality, especially for small objects, by both algorithms, an overall over-sampling with at least 8x8 pixel subdivisions should be used in the case of ray tracing. For such pixel subdivisions our beam tracing is between 1.76 and 2.46 times faster than ray tracing.

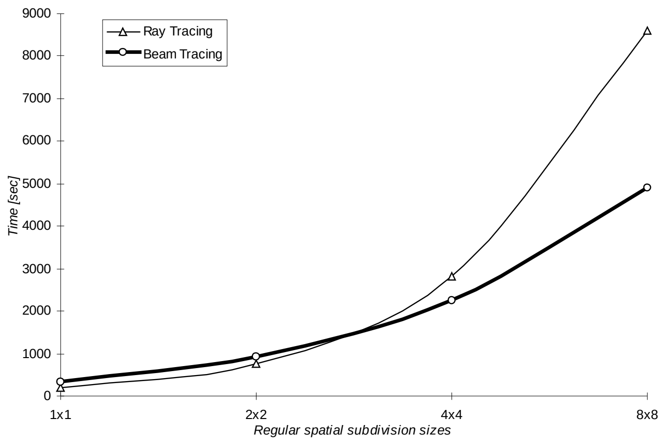

a: *Virtual town (1519 polyhedra).*

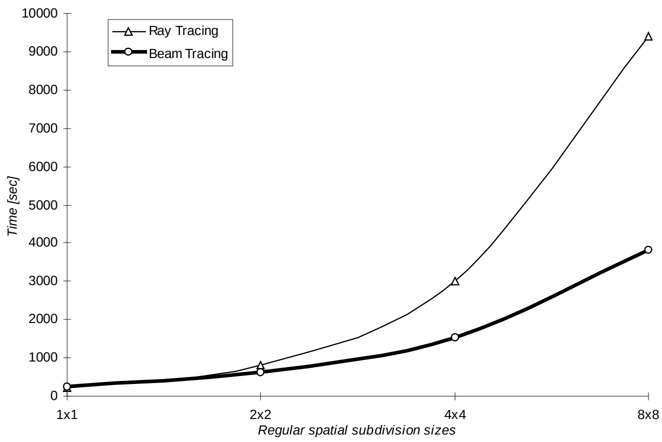

b: *2060 random placed cubes.*

Figure 14*: Time comparison between the ray tracing and our beam tracing for a 70x70x70 regular spatial subdivision and a 1024x1024 pixels image with different pixel subdivisions.*

4.3 Soft shadows

With small volumic light sources, there is no graphical difference between our beam tracing and the stochastic ray tracing but our beam tracing is more time consuming. With large volumic light sources, the stochastic ray tracing uses a lot of rays to produce good quality soft shadows. So, it becomes too expensive to be used in this case but our beam tracing can produce good quality soft shadows (***image 4***) with a more reasonable cost.

5. Conclusion and future works

This method, which can be considered as a beam-ray tracing with adaptive image subdivisions, is an efficient technique with general and robust antialiasing for polyhedral scenes. Particularly, small objects and small shadows are detected and processed precisely. Usual linear approximations or complex computations for refractions used in similar beam tracers are avoided with this method. Moreover, this method is well adapted to texture antialiasing with no over-sampling.

Pyramidal shape beams are used as a bounding volume to detect uniform and ambiguous regions. Opposite to other beam tracers, no explicit beam-object intersection computation is needed. This is the main advantage of our beam tracer compared to similar methods using complex beam-object intersection and 3D clipping computations.

The extension of our beam tracing method to some non-polyhedral scenes is possible because of the absence of explicit beam-object intersection computations. This is, in particular, the case of scenes composed of geometric entities (spheres, cylinders, cones, ...) whose positions relative to pyramidal beams can be simply determined. Thus, our beam tracer can be extended to CSG scenes. An extension of our beam tracer for visualizing CSG scenes with no reflection and no refraction is developed in [27]. A general extension of this method to CSG scenes including reflections and refractions is more complicated. It is the subject of future works.

Our beam tracer, in which the beams are used as pyramidal bounding boxes, is well adapted to decrease the cost of form factor computations in radiosity algorithms. This is another subject of future works.

Acknowledgements: We would like to thank the *Conseil Régional du Limousin* for its financial support for this work.

References

1. D. GHAZANFARPOUR and B. PEROCHE, Antialiasing by Successive Steps with a z-buffer, *Proceedings of Eurographics' 89*, Hambourg, 235-244 (1989).
2. T. WHITTED, An Improved Illumination Model for Shaded Display, *Communication of the ACM*, 23(6), 343-349 (1980).
3. J. ARGENCE, Antialiasing for Ray Tracing Using CSG Modelling, CG International'88, *New Trends in Computer Graphics,* 199-208 (1988).
4. R. COOK, Stochastic Sampling in Computer Graphics, *ACM Transactions on Graphics,* 5(1), 51-72 (1986).
5. D. MITCHELL, Generating Antialiased Images at Low Sampling Densities, *Computer Graphics,* 21(4), 65-72 (1987).
6. J. PAINTER and K. SLOAN, Antialiased Ray Tracing by Adaptative Progressive Refinement, *Computer Graphics*, 23(3), 281-288 (1989).
7. J. AMANATIDES, Ray Tracing with Cones, *Computer Graphics*, 18(3), 129-135 (1984).
8. P. HECKBERT and P. HANRAHAN, Beam Tracing Polygonal Objects, *Computer Graphics*, 18(3), 119-127 (1984).
9. D. KIRK, The Simulation of Natural Features Using Cone Tracing, *The Visual Computer,* 3(2), 63-71 (1987).
10. M. SHINYA, T. TAKAHASHI and S. NAITO, Principals and Applications of Pencil Tracing, *Computer Graphics*, 21(4), 45-54 (1987).
11. D. GHAZANFARPOUR, Visualisation réaliste par lancer de pyramides et subdivision adaptative, *Proceedings of MICAD 92*, PARIS, 167-181 (1992).
12. J. WARNOCK, A Hidden-Surface Algorithm for Computer Generated Half-Tone Pictures, *University of Utah, TR 4-15*, NTIS AD-753 671 (1969).
13. A. FUJIMOTO, T. TANAKA, and K. IWATA, ARTS: Accelearted Ray-Tracing System, *IEEE Jouranl of Computer Graphics and Applications,* 6(2), 16-26 (1986)
14. J. AMANATIDES and A. WOO, A Fast Voxel Traversal Algorithm for Ray-Tracing, *Proceedings of Eurographics Conference*, 27-38 (1987).
15. J. G. CLEARY and G. WYVILL, Analysis of an Algorithm for Fast Ray Tracing Using Uniform Space Subdivision, *Journal of the Visual Computer*, 4(1), 65-83 (1988).
16. A. GLASSNER, Space Subdivision for Fast Ray Tracing, *IEEE Journal of Computer Graphics and Applications,* 4(5), 15-22 (1984).
17. H. SAMET, Implementing Ray Tracing with Octrees and Neighbor Finding, *Computers and Graphics*, 4(13), 445-460 (1989).
18. J. SPACKMAN and P. WILLIS, The {SMART} Navigation of a Ray Through an Oct-Tree, *Computers and Graphics*, 2(15), 185-194 (1991).
19. R. ENDL and M. SOMMER, Classification of Ray-Generators in Uniform Subdivisions and Octrees for Ray Tracing, *Comupter Graphics Forum*, 13(1), 3-19 (1994).
20. H. K. CHOI, C. M. KYUNG, PYSHA - A Shadow-Testing Acceleration Scheme for Ray-Tracing, *Computer-Aided Design*, 24(2), 93-104 (1992).
21. D. GHAZANFARPOUR and B. PEROCHE, A High Quality Fitering Using Forward Texture Mapping, *Computers & Graphics*, 15(4), 569-577 (1991).
22. L. WILLIAMS, Pyramidal Parametrics, *Computer Graphics*, 17(3), 1-11 (1983).
23. M. GANGNET and D. GHAZANFARPOUR, Techniques for Perspective Mapping of Plane Textures, *International Electronic Image Week*, CESTA, Biarritz, 29-35 (1984).
24. D. GHAZANFARPOUR and J. M. DISCHLER, Spectral Analysis for Automatic 3D Texture Generation, *Computers &* Graphics, 19(3), 413-422 (1995).
25. D. GHAZANFARPOUR, J.M. DISCHLER, Generation of 3D Texture Using Multiple 2D Models Analysis, *Computer Graphics Forum* (*N° spécial EUROGRAPHICS' 96*), 15(3), 311-323 (1996).

26. A. WOO, P. POULIN, and A. FOURNIER, A Survey of Shadow Algorithms, *IEEE Computer Graphics & Applications*, 13-32 (1990).
27. J. M. HASENFRATZ and D. GHAZANFARPOUR, Rendering CSG Scenes with General Antialiasing, *CSG'96*, Winchester, 275-289 (1996).

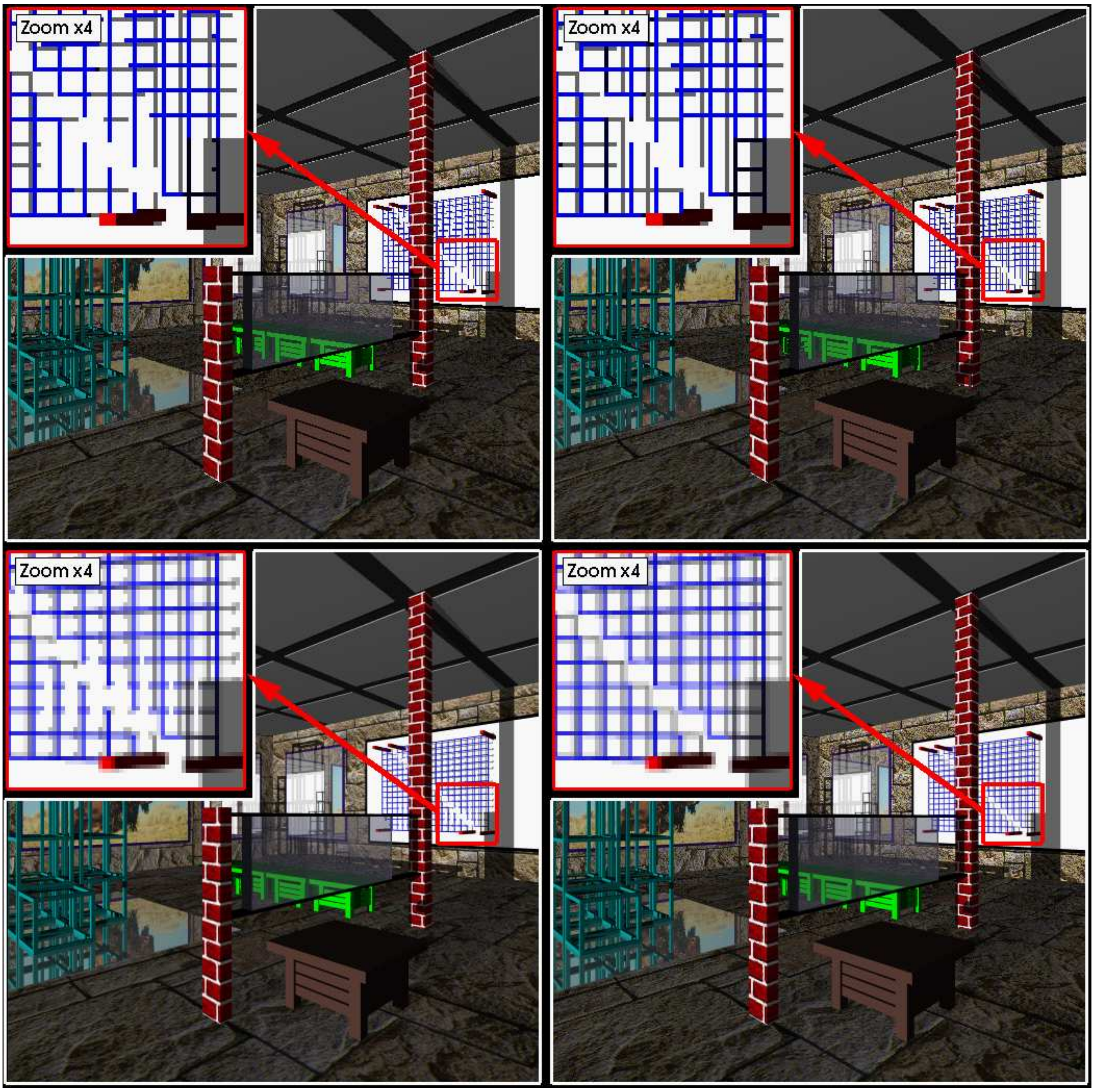

***Image 1:** The room test scene with different aliasing problems, in particular with small objects.*
***(top-left)** Ray tracing with no antialiasing. **(top-right)** Beam tracing with no antialiasing.*
***(bottom-left)** Ray tracing with adaptative over-sampling (8x8 rays per pixel).*
***(bottom-right)** Beam tracing with at most 8x8 sub-beams.*

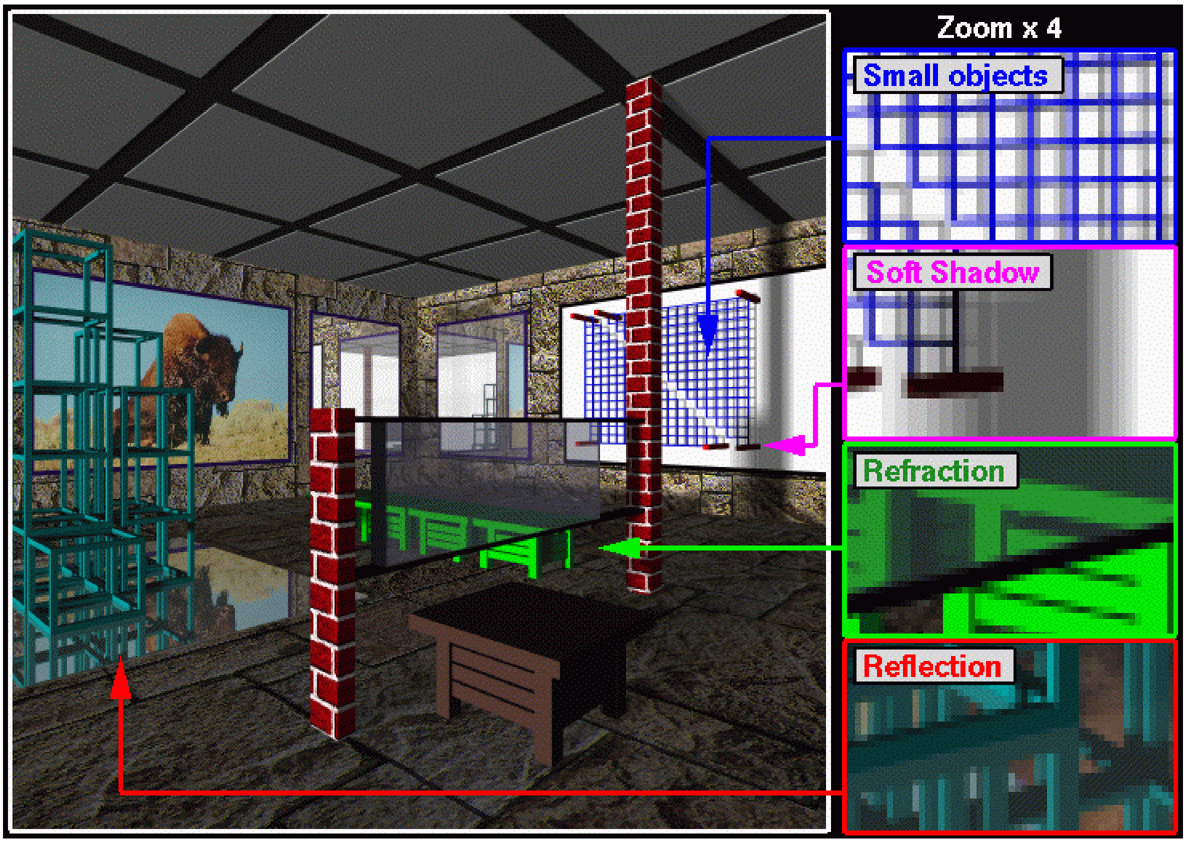

Image 2: *Small objects detection and different possible effects produced by our beam tracing.*

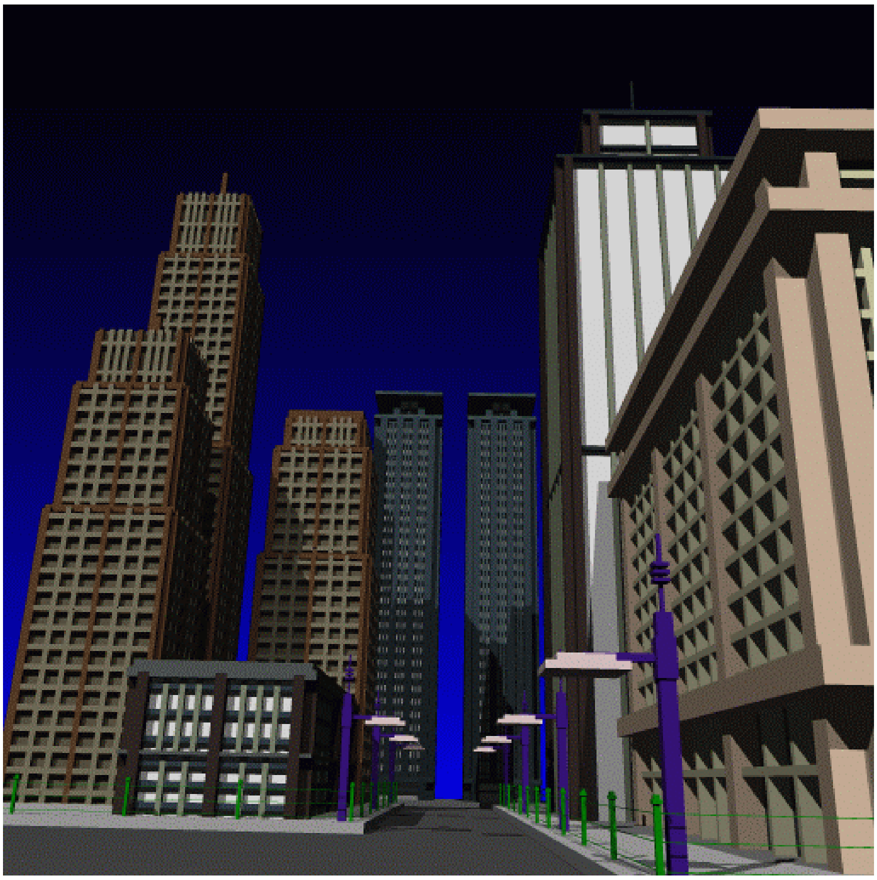

Image 3*: The virtual town test scene produced by our beam tracing with a maximum of 8x8 sub-beams per pixel and with punctual light sources. This scene is used in the computational time comparison.*

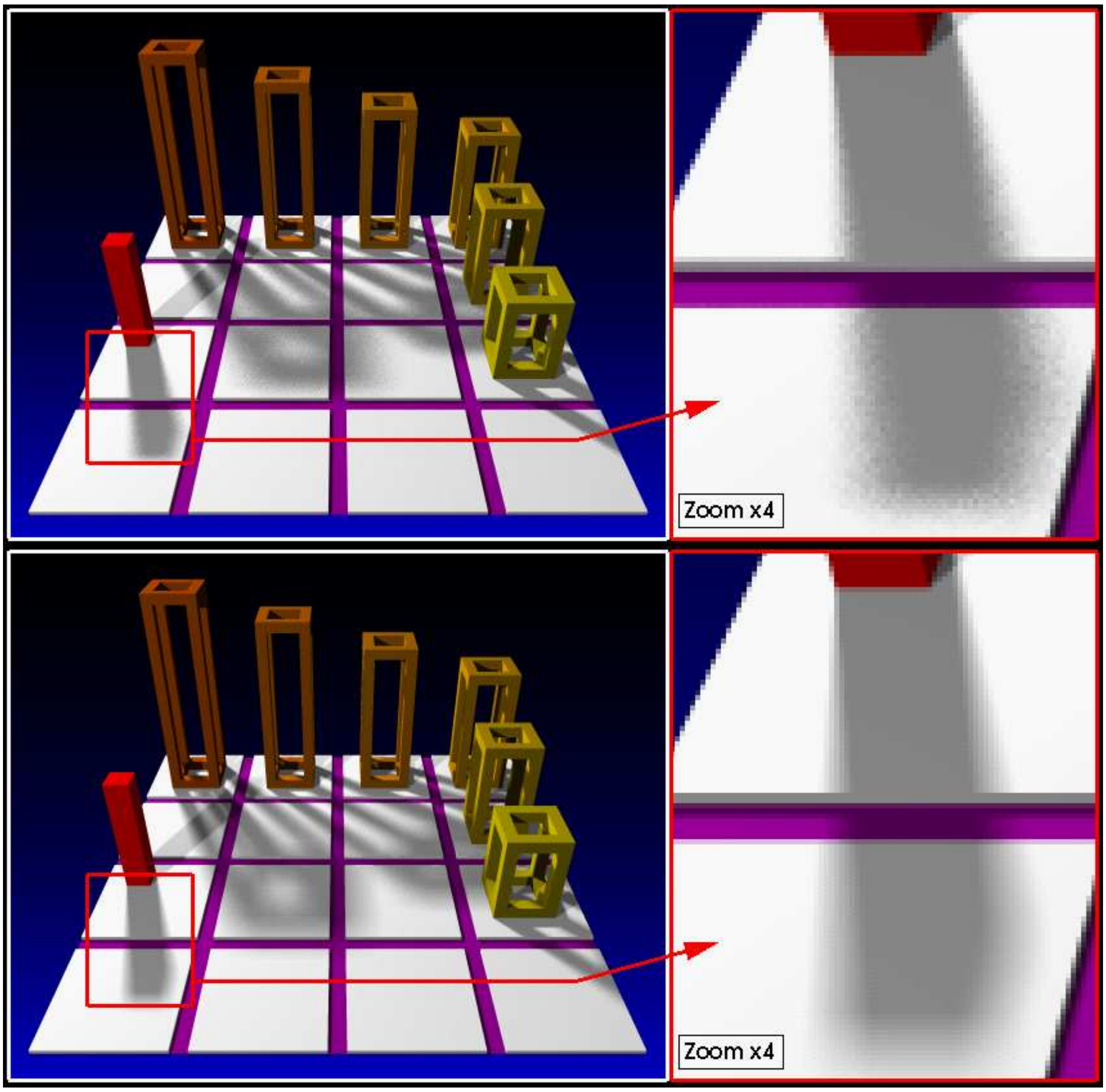

***Image 4**: The seven pillars test scene with soft shadows in the case of a large light source.*
***(top)** Soft shadows with a stochastic ray tracing and 8x8 rays per pixel and its zoom.*
***(bottom)** Soft shadows produced by the beam tracing with at most 8x8 sub-beams and its zoom.*